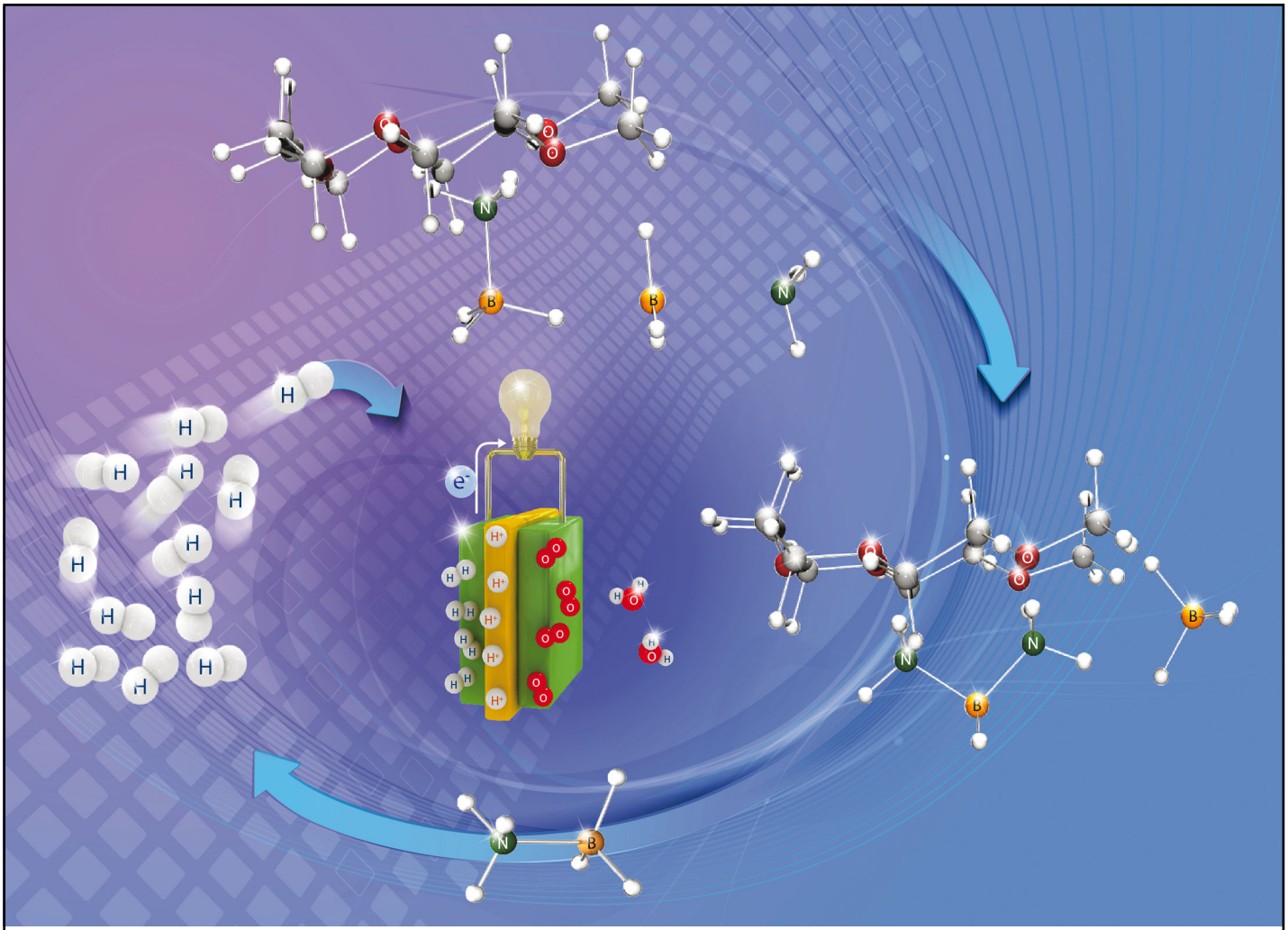

Showcasing research from the group of Chang Won Yoon at the Korea Institute of Science and Technology

Title: Metal-free, polyether-mediated H_2-release from ammonia borane: roles of hydrogen bonding interactions in promoting dehydrogenation

A metal-free method for H_2-release from ammonia borane with the addition of polyethers would be helpful for the development of feasible hydrogen storage systems.

As featured in:

See Yongmin Kim *et al.*, *Phys. Chem. Chem. Phys.*, 2013, **15**, 19584.

www.rsc.org/pccp

Registered Charity Number 207890

PCCP

RSC Publishing

PAPER

View Article Online
View Journal | View Issue

Metal-free, polyether-mediated H_2-release from ammonia borane: roles of hydrogen bonding interactions in promoting dehydrogenation†

Cite this: *Phys. Chem. Chem. Phys.*, 2013, **15**, 19584

Yongmin Kim,[a] Hyunjae Baek,[a] Jin Hee Lee,[a] Shinyoung Yeo,[a] Kibum Kim,[a] Son-Jong Hwang,[b] Bit Eun,[a] Suk Woo Nam,[ac] Tae-Hoon Lim[ac] and Chang Won Yoon*[ad]

Received 21st June 2013,
Accepted 29th July 2013

DOI: 10.1039/c3cp52591k

www.rsc.org/pccp

Polyetheral additives were found to be efficient promoters to enhance the rate of H_2-release from ammonia borane (AB) at various temperatures. In particular, tetraethylene glycol dimethyl ether (T4EGDE, 29 wt% relative to AB + T4EGDE) exhibited significantly improved activities for AB dehydrogenation, with the material-based hydrogen storage capacity of 10.3 wt% at 125 °C within 40 min. *In situ* FT-IR spectroscopy indicated the formation of B-(cyclodiborazanyl)amino-borohydride (BCDB), borazine, and μ-aminodiborane as gaseous byproducts. In addition, ^{11}B nuclear magnetic resonance (NMR) spectroscopy further revealed that diammoniate of diborane (DADB) was initially formed to give polyaminoborane as liquid and/or solid spent-fuel, consistent with previous reports. Density Functional Theory (DFT) calculations suggested that hydrogen bonding interactions between AB and a polyetheral promoter initially played an important role in increasing the reactivity of B–H bonds of AB by transferring electron density from oxygen atoms of the promoter into B–H bonds of AB. These partially activated, hydridic B–H bonds were proposed to help promote the formation of diammoniate of diborane (DADB), which is considered as a reactive intermediate, eventually enhancing the rate of H_2-release from AB. In addition, our *in situ* solid state ^{11}B magic angle spinning (MAS) NMR measurements further confirmed that the rate of DADB formation from AB with a small quantity of T4EGDE was found to be much faster than that of pristine AB even at 50 °C. This metal-free method for H_2-release from AB with an added, small quantity of polyethers would be helpful to develop feasible hydrogen storage systems for long-term fuel cell applications.

Introduction

As pressure continues to build for solutions to energy and environmental issues, the need to develop clean, efficient, and sustainable energy systems is becoming increasingly urgent.[1] Fuel cells represent highly promising power generators that meet such demands as long as the hydrogen they need can be produced in a renewable manner.[2,3] In this context, high-density hydrogen storage materials are necessary not only to store excess energy generated from the renewable sources in molecular form for future utilization but also to develop power fuel cells that enable long-term applications.[4] Among various types of hydrogen storage materials, chemical hydrogen storage materials have received considerable attention because they can release hydrogen under mild conditions with high gravimetric hydrogen storage capacity that may satisfy the guidelines established for transportation applications as determined by the US Department of Energy.[5,6] In addition, significant efforts have recently been made to demonstrate feasible chemical hydrogen storage systems for uses in portable power packs and unmanned aerial vehicles (UAVs).[7–9] However, to further improve hydrogen storage capacities of various chemical hydrogen storage materials for realization of economically viable systems, a better understanding of the H_2-release mechanism for these materials is required.

Due to its high hydrogen storage capacity (19.6 wt% H_2), ammonia borane (AB) is recognized as a promising candidate in this development process. In addition, the potential regenerability

[a] *Fuel Cell Research Center, Korea Institute of Science and Technology, 39-1 Hawolgok-dong, Sungbuk-gu, Seoul 136-791, Republic of Korea. E-mail: cwyoon@kist.re.kr*
[b] *Division of Chemistry and Chemical Engineering, California Institute of Technology, Pasadena, California 91125, USA*
[c] *Green School, Korea University, 145 Anam-ro, Seongbuk-gu, Seoul 136-791, Republic of Korea*
[d] *Department of Clean Energy and Chemical Engineering, University of Science and Technology, Daejeon, Republic of Korea*

† Electronic supplementary information (ESI) available: Details of the reaction conditions and Cartesian coordinates of the optimized geometries. See DOI: 10.1039/c3cp52591k

that has recently been demonstrated using liquid ammonia and hydrazine as a reducing agent,[10] further strengthens the potential of this material as an energy carrier. The AB molecule possesses protonic N–H (δ^+) and hydridic B–H (δ^-) bonds, and this electronic property allows hydrogen release under mild conditions.[11] In general, when compared to AB hydrolysis, the thermal decomposition of AB provides much higher gravimetric hydrogen storage density and is thus particularly desirable for long-term and/or transportation applications. Thermolysis of pristine AB, however, has exhibited slow dehydrogenation kinetics at 90 °C with an induction period[12] for potential fuel cell applications. In this regard, the development of an efficient procedure for AB dehydrogenation under mild conditions has attracted significant attention for its potential to enable chemical hydrogen storage with high energy density.

Significant efforts have already been made to accelerate H_2-release from AB using a number of homogeneous, precious metal catalysts including Rh,[13] Ir,[14–18] Ru,[19–23] and Ni (Scheme 1a).[24–27] In addition, an economically viable Fe-based catalyst has recently been developed for practical applications; Baker *et al.*[28] reported Fe-based complexes possessing mixed amido/phosphine ligands that released *ca.* 1.7 equiv. of H_2 over a period of hours at 60 °C. Along with these approaches, a number of novel strategies using non-metal based additives have also been utilized to address this issue (Scheme 1b); for example, Autrey and coworkers found that AB confined at a silica-based mesoporous material, SBA-15, lowered dehydrogenation temperature with reduced amounts of the borazine byproduct.[29] Moreover, the addition of trace quantities of diammoniate of diborane (DADB) to AB was found to reduce the induction period or onset temperature for H_2-release.[12] In addition, use of activated boron nitride (BN) was also reported to decrease the onset temperature of H_2 production.[30,31] More recently, Sneddon and coworkers demonstrated that an additive of proton sponge[32] (PS, *ca.* 5 wt%) or Verkade's base[33] could enhance the rate and extent of H_2-release from AB at 85 °C. Furthermore, ionic liquids[34,35] (ILs, 50 wt%) and mixtures of PS/IL[32] (IL, 50 wt%) have been found to significantly improve the rate and extent of H_2-release from AB, with >2 equiv. of H_2 being released under mild conditions. Similarly, a mixture of AB and tetraethylene glycol dimethyl ether (T4EGDE) (50 : 50, wt%) was reported to accelerate the dehydrogenation reaction.[34] Theoretical studies have also been conducted to understand the thermodynamics[36,37] and kinetics[38,39] of the AB dehydrogenation. Despite these improvements, however, the reduction of such promoters is still needed to achieve a high energy density from AB for practical applications.[40] Furthermore, understanding the roles of additives is another prerequisite for developing hydrogen generators based on such mixtures. To the best of our knowledge, no detailed studies have been reported to scrutinize the potential functions of polyetheral additives for improving AB dehydrogenation.

We report here on metal-free, H_2-release from AB, extending previous approaches utilizing chemical additives. We demonstrate that mixtures of AB and polyetheral promoters can release *ca.* 2 equiv. of H_2 with enhanced rates and extents even in the absence of metal catalysts under mild conditions. In particular, a mixture of AB and T4EGDE (71 : 29, wt%) released >2 equiv. of hydrogen at 125 °C within 40 min, which corresponds to a material-based H_2 storage capacity of >10 wt% that may meet the requirement for fuel cell applications requiring long-term operation. In addition, Density Functional Theory (DFT) methods in combination with the experimental results achieved by *in situ* solid state ^{11}B magic angle spinning (MAS) nuclear magnetic resonance (NMR) spectroscopy were employed to shed light on the possible roles of the polyetheral additives in promoting AB dehydrogenation and suggest that the added polyetheral promoters may initially accelerate the formation of DADB from AB to ultimately enhance the rate of dehydrogenation.

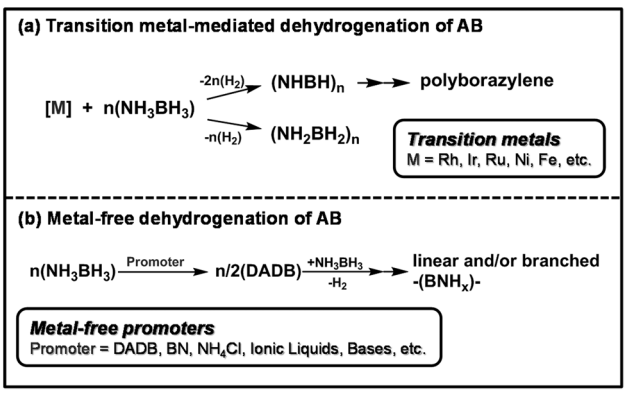

Scheme 1 Previous approaches for AB dehydrogenation: (a) transition metal mediated dehydrogenation of AB and (b) metal-free dehydrogenation of AB.

Results and discussion

H_2-release properties of the mixtures of AB and a polyetheral promoter

Thermolysis of AB (0.12 g, 4.0 mmol) produced hydrogen at 85 °C with a series of polyetheral promoters, as depicted in Chart 1. The AB solids released H_2 slowly with an induction period of about 120 min and yielded 0.3 eq. of H_2 within 180 min (Fig. 1), which is consistent with previous results.[12] In contrast, upon utilization of the DEGDE, T3EGDE, and T4EGDE additives (AB : promoter = 4.0 : 0.50, mmol), immediate H_2-release from AB was observed at 85 °C and exhibited much faster rates of dehydrogenation than those from the pristine AB solids with the order of T4EGDE > T3EGDE > DEGDE > EGDE (Fig. 1a); *i.e.*, the EGDE, DEGDE, T3GDE, and T4EGDE promoters produced 0.9, 1.1, 1.6, and 1.8 equiv. of H_2 with respect to AB

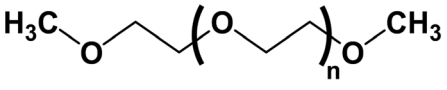

n=0 : Ethylene glycol dimethyl ether (EGDE)
n=1 : Diethylene glycol dimethyl ether (DEGDE)
n=2 : Triethylene glycol dimethyl ether (T3EGDE)
n=3 : Tetraethylene glycol dimethyl ether (T4EGDE)

Chart 1 Structures of a series of polyetheral promoters.

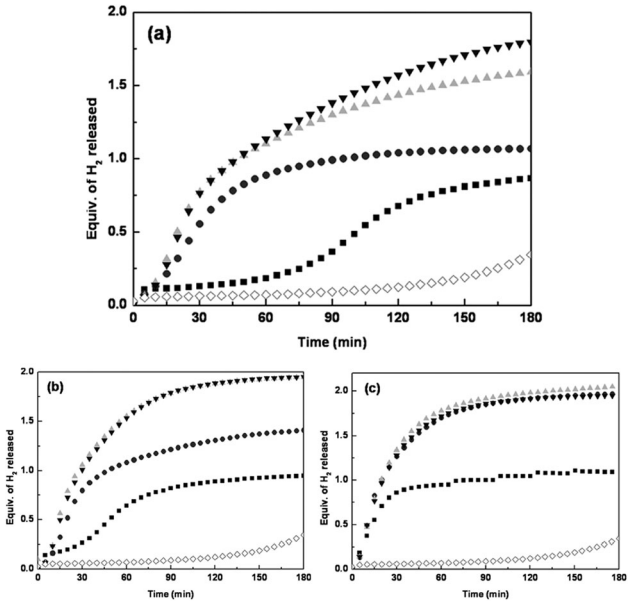

Fig. 1 H_2-release from AB at 85 °C in the presence of different molar ratios of the promoters (EGDE, ■; DEGDE, ●; T3EGDE, ▲; T4EGDE, ▼; and no promoter, ◇): (a) AB : promoter = 4.0 : 0.5; (b) AB : promoter = 4.0 : 1.0; (c) AB : promoter = 4.0 : 2.3. Detailed quantities of AB and promoters are listed in Table S1 in the ESI.†

within 180 min. The EGDE additive showed slight enhancement for AB dehydrogenation with a reduced induction period of *ca.* 60 min under the same conditions. In addition, the rates of AB dehydrogenation appear to be associated with the molar ratio of AB and a promoter, and the rates of H_2-release with T4EGDE, T3EGDE, and DEGDE became identical as the amounts of promoters increased (Fig. 1b and c).

Liquid and/or solid spent-fuels after the thermolysis of AB in the presence of T4EGDE at 85 °C were further analyzed by ^{11}B NMR spectroscopy. Consistent with previous results,[41–43] ^{11}B NMR spectroscopy revealed that liquid/solid byproducts containing sp^3 boron (*e.g.*, polyaminoborane, PAB) and DADB were formed (Fig. 2a); *i.e.*, peaks centered at δ = −11 ppm (BH_2^+) and at δ = −36 ppm (BH_4^-) come from DADB while those centered at δ = −5 ppm (BH), at δ = −11 ppm (BH_2) and at δ = −22 ppm (BH_3) resulted from linear and/or branched polyaminoborane.[41–43] Moreover, waste-fuels containing B–O bonds (δ = 1–20 ppm)[43,44] were not visible in the ^{11}B NMR spectra. Other EGDE, DEGDE, and T3EGDE additives also afforded similar product distributions upon AB dehydrogenation at 85 °C (Fig. 2b), as evidenced by ^{11}B NMR spectroscopic studies. Since no DADB was yielded within 60 min upon heating of the pristine AB solid at 85 °C under our reaction conditions (Fig. S1†), the rates of DADB formation from AB in the presence of polyetheral promoters are much faster than those without the promoters.

The FT-IR spectra of the gaseous byproducts obtained *in situ* during AB dehydrogenation in the presence of the T4EGDE additive exhibited the IR frequencies at 3300 cm^{-1} (N–H) and at 2400 cm^{-1} (B–H) after 30 min (Fig. 3a). This gaseous molecule was likely B-(cyclodiborazanyl)amino-borohydride (BCDB),

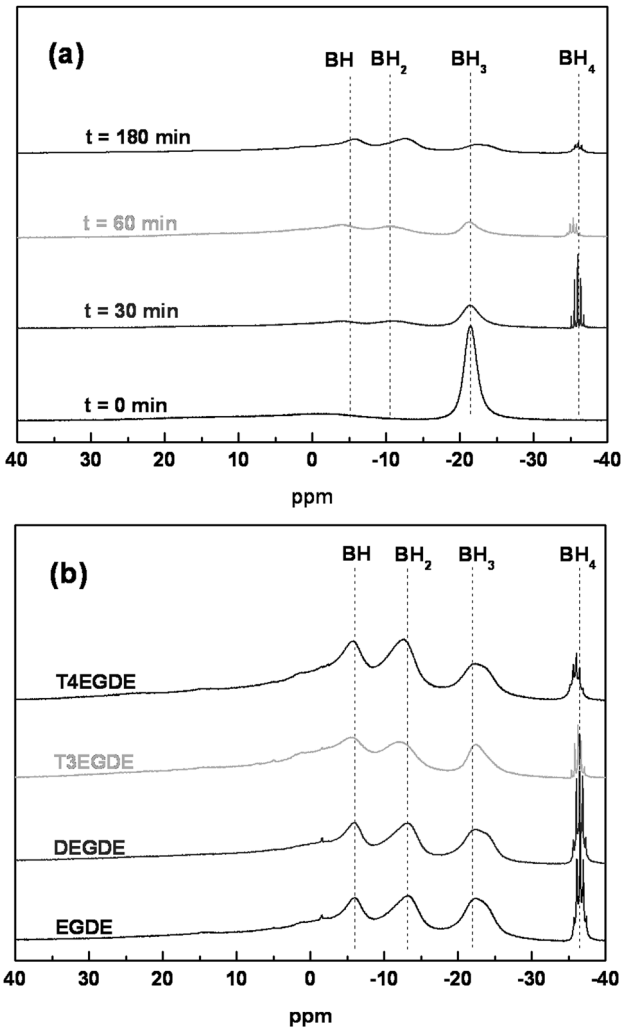

Fig. 2 (a) ^{11}B NMR spectra of spent-fuels following the dehydrogenations of AB (0.12 g, 4.0 mmol) at 85 °C in the presence of T4EGDE (0.050 g, 0.23 mmol; 29 wt% with respect to AB + T4EGDE) with time. (b) ^{11}B NMR spectra of spent-fuels following the dehydrogenation of AB (0.12 g, 4.0 mmol) at 85 °C in the presence of EDGE, DEGDE, T3EGDE, and T4EGDE (0.050 g; 29 wt% with respect to AB + promoters) after 180 min. The NMR spectra were obtained by dissolving the residues in T4EGDE (0.5 g).

which was first identified by Pons *et al.*,[45] and the observed IR frequencies were in good agreement with the one calculated using the DFT-optimized geometry of BCDB (Fig. S2†). No peaks corresponding to ammonia,[46] centered at around 1000 cm^{-1}, were detected under the conditions employed. Upon increasing the dehydrogenation temperature from 85 °C to 105 °C, borazine ($B_3N_3H_6$) with the IR frequencies at ~3500 cm^{-1} (N–H) and at ~2500 cm^{-1} (B–H) was clearly observed in the FT-IR spectra along with BCDB (Fig. 3b). In the case of temperatures of >85 °C, a small quantity of μ-aminodiborane was also observed (Fig. S2†). The formation of BCDB, borazine, and μ-aminodiborane as gaseous byproducts was again confirmed by ^{11}B NMR spectroscopy (Fig. S3†).

The quantity of the polyetheral promoter could potentially influence the rate and extent of H_2-release from AB. Indeed, an optimized quantity of T4EGDE (2.0 mmol) with respect to AB

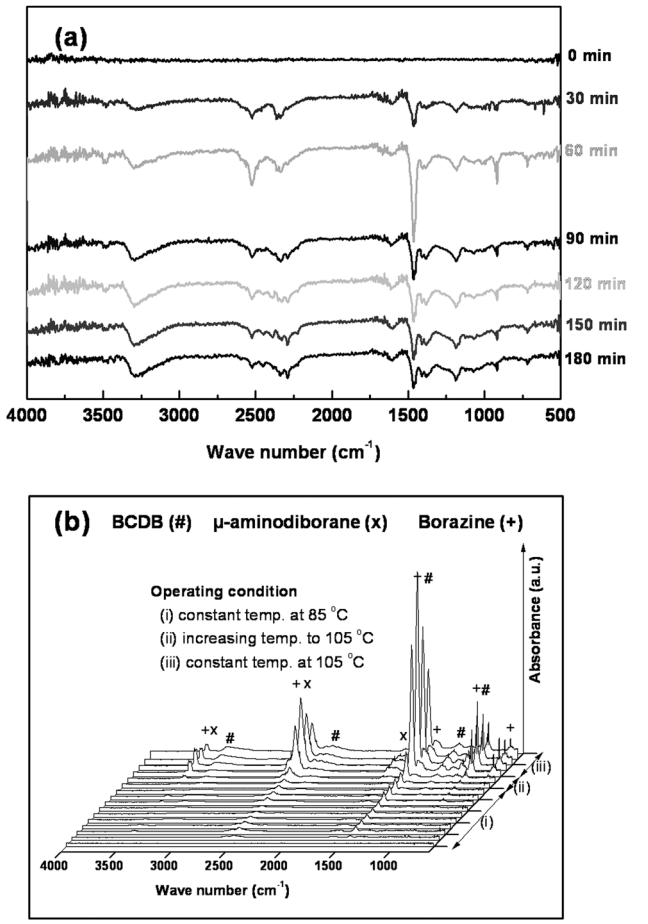

Fig. 3 (a) *In situ* FT-IR spectra of the gaseous byproducts produced during the dehydrogenation of AB (0.12 g, 4.0 mmol) at 85 °C in the presence of T4EGDE (0.050 g, 0.23 mmol) with time. (b) *In situ* FT-IR spectra following the AB dehydrogenation in the presence of T4EGDE (0.050 g, 0.23 mmol) upon increasing the temperature from 85 °C to 105 °C.

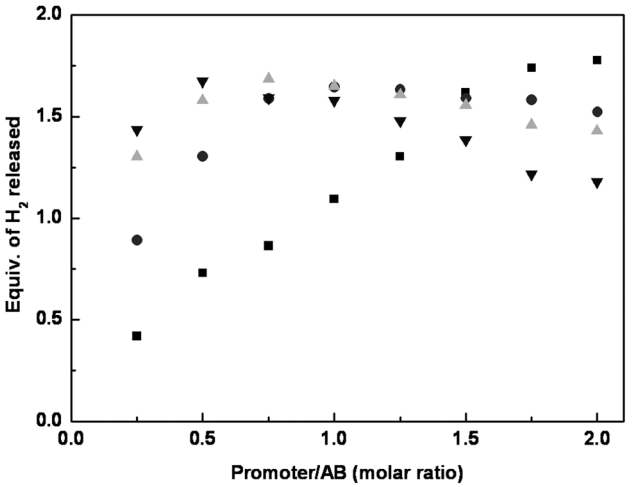

Fig. 4 H_2-release from AB (4.0 mmol) at 85 °C in the presence of different amounts of promoters: EGDE (■), DEGDE (●), T3EGDE (▲), and T4EGDE (▼). The quantities of H_2 labeled at the *Y*-axis were measured after 60 min. Detailed quantities of AB and promoters are listed in Table S2 in the ESI.†

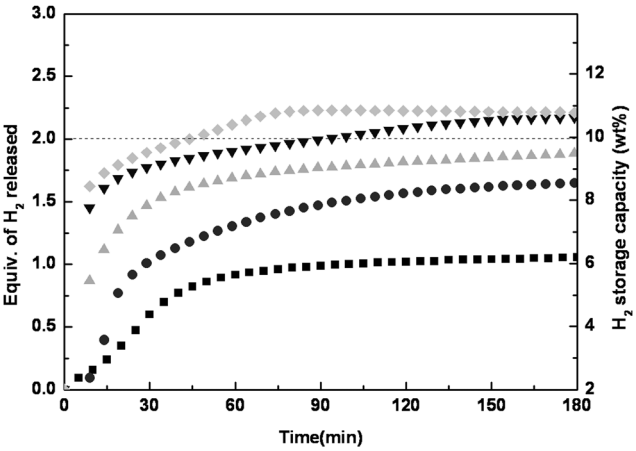

Fig. 5 Temperature dependence of the H_2-release from AB (0.12 g, 4.0 mmol) in the presence of T4EGDE (0.050 g, 0.23 mmol): (■) 85 °C, (●) 95 °C, (▲) 105 °C, (▼) 115 °C, and (♦) 125 °C.

(4.0 mmol) was found for dehydrogenation; that is, more than 2.0 mmol of T4EGDE decreased the rate of H_2 production from AB under the same conditions (Fig. 4 and Fig. S4d†). Likewise, other promoters (EGDE, DEGDE, and T3EGDE) were found to have optimized quantities for AB hydrogenation (Fig. 4 and Fig. S4a–c†). These results are in line with the previous discovery that the rate of AB dehydrogenation with T3EGDE was dependent upon the quantity of the promoter used.[43] The dependence of the H_2-release rate on additive quantity implies that excess amounts of a polyetheral additive retard the formation of H_2 by suppressing the intermolecular interactions between two ABs (*vide infra*).

The rate of AB dehydrogenation is further found to be dependent on temperature (Fig. 5). Increases in temperature raised the rate of H_2-release from the mixtures of AB and T4EGDE (4.0 : 0.23, mol%; 71 : 29, wt%). For instance, the mixture of AB and T4EGDE afforded *ca.* 0.2, 0.5, 1.2, 1.6, and 1.8 equiv. of hydrogen relative to AB at 85 °C, 95 °C, 105 °C, 115 °C, and 125 °C, respectively, for 15 min. In particular, 2.2 equiv. of H_2 with respect to AB was released upon dehydrogenation of a mixture of AB and T4EGDE at 125 °C within 40 min (Fig. 5). The increased H_2 yield upon raising temperatures >95 °C was attributable to the formation of polyborazylene as well as borazine (Fig. S5†). This quantity of hydrogen corresponds to 10.3 wt% of material-based hydrogen storage density.[47] Given that the temperature of 125 °C can readily be achieved autothermally during AB dehydrogenation,[7] the mixture of AB with small amounts of added T4EGDE (29 wt%) as a promoter could satisfy the criteria for fuel cell applications requiring high gravimetric density for H_2 storage.

Understanding the potential role of a polyetheral promoter

Since the added polyethers promoted the rates of H_2-release from AB, it was hypothesized that oxygen atoms of the polyetheral additives were responsible for the increased rates of AB dehydrogenation. To elucidate the effect of the oxygen atoms in the polyetheral promoters, we used pentadecane that possesses

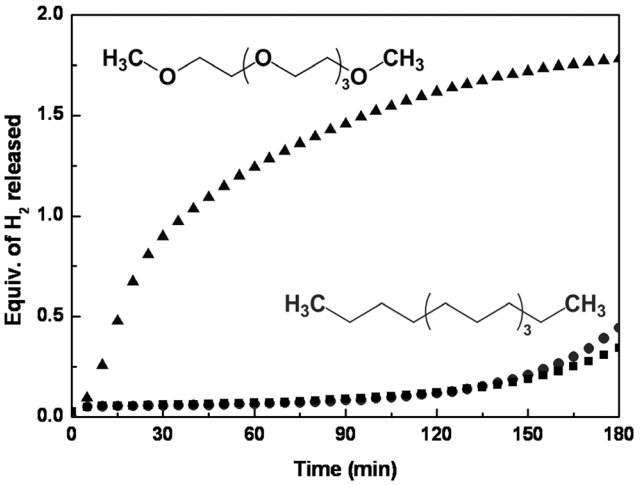

Fig. 6 Comparison of the H_2-release from AB (0.12 g, 4.0 mmol) in the presence of T4EGDE (0.11 g, 0.50 mmol) or pentadecane (0.11 g, 0.50 mmol) at 85 °C: (▲) T4EGDE, (●) pentadecane, and (■) no promoter.

no oxygen atoms but has a comparable chain length to T4EGDE. Compared to those without a promoter, the rate and extent of H_2-release from AB in the presence of pentadecane exhibited negligible enhancement (Fig. 6). The accelerated H_2-release from AB thus likely resulted from the interactions between AB and the oxygen atoms in T4EGDE.

AB has previously been shown to interact with 18-crown-6 *via* hydrogen bonding interactions to form the AB·18-crown-6 adduct.[48,49] Since the T4EGDE additive can be considered as a 18-crown-6-type molecule without a "CH_2–O–CH_2" unit(s) (Chart 2), it is conceivable that the oxygen atoms of the T4EGDE promoter likewise interact with N–H bonds at AB through hydrogen bonding. In this context, potential interactions between oxygen atoms of this polyetheral promoter and the N–H bonds at AB were further explored by DFT methods. Since the previously reported crystal structure of the AB·18-crown-6 adduct showed the presence of three hydrogen bonds between three N–H bonds and three oxygen atoms in 18-crown-6,[48,49] analogous interactions between AB and a polyetheral promoter were considered.

The DFT-optimized AB·T4EGDE (**1**) adduct exhibited three hydrogen bonding interactions (O···H–N, Fig. 7a) with the following geometrical parameters: H1···O1 (2.078 Å), H2···O5 (2.063 Å), H3···O3 (2.079 Å), N–H1–O1 (175°), N–H2–O5 (168°), and N–H3–O3 (175°). Stabilization energy of **1** was calculated to be 23.5 kcal mol^{-1} with respect to AB + T4EGDE (Table S3†). Other promoters, T3EGDE and DEGDE, can also interact with

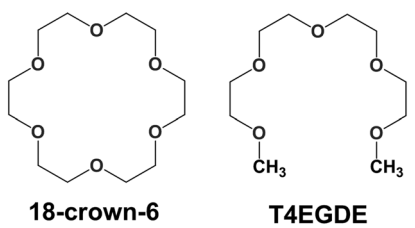

Chart 2 Comparison of the structure of 18-crown-6 and T4EGDE.

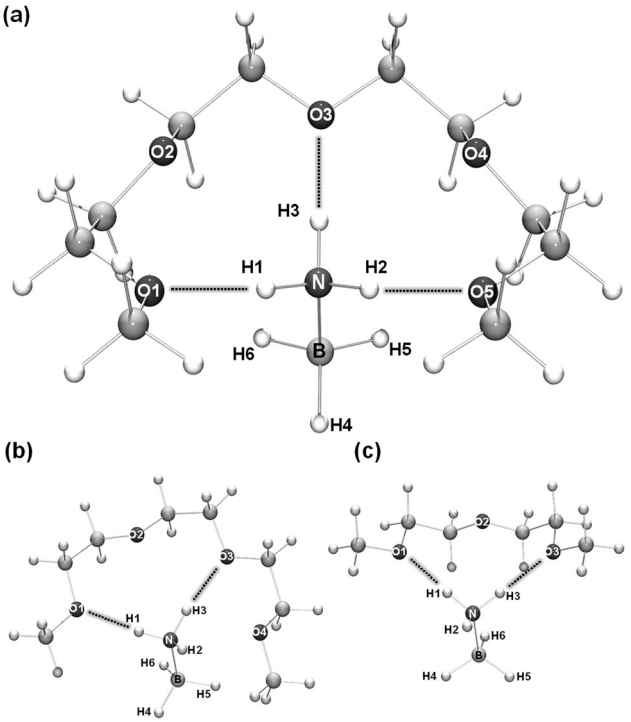

Fig. 7 DFT-optimized geometries for AB·L adducts (L = promoters), calculated by the B3LYP/6-31+G(d,p) level of theory (dark gray, carbon; light gray, hydrogen): (a) T4EGDE, (b) T3EGDE, and (c) DEGDE. Dotted lines represent hydrogen bonding interactions.

AB *via* hydrogen bonding to yield more stable complexes, AB·T3EGDE (**2**) and AB·DEGDE (**3**), with 19.0 kcal mol^{-1} and 15.9 kcal mol^{-1} of stabilization energies, respectively (Fig. 7b and c; Table S3†). No AB·EGDE adduct possessing well-defined interactions was found presumably due to insufficient amounts of oxygen atoms within the EGDE promoter. Selected geometrical parameters for **1**, **2** and **3** are summarized in Table 1.

These hydrogen bonding interactions present at **1–3** could influence the charge density of the B–H bonds at AB *via* charge transfer since the oxygen atoms in the polyethers are charge donors in the hydrogen bonding pairs. Since Mulliken charge analyses were previously employed to understand the bonding nature of AB, hydrazine, $LiNH_2BH_3$, and $Ca(NH_2BH_3)_2$ involving hydrogen bonding interactions,[50–52] we initially conducted Mulliken charge analyses of these adducts in the gas phase to elucidate the roles of the hydrogen bonding interactions in enhancing the rate of H_2-release. Compared to that of AB (δ = −0.077), the average charge of the B–H bonds in **1**

Table 1 Selected geometrical parameters of the optimized complexes **1–3**

	AB·T4EGDE (**1**)	AB·T3EGDE (**2**)	AB·DEGDE (**3**)
B–N (Å)	1.628	1.631	1.641
H1–O1 (Å)	2.078	2.037	2.039
H3–O3 (Å)	2.063	2.042	2.039
H2–O5 (Å)	2.079	—	—
N–H1–O1 (°)	175	175	176
N–H3–O3 (°)	168	162	176
N–H2–O5 (°)	175	—	—

Table 2 Calculated Mulliken and NBO charges of the optimized complexes, **1–3**

	Charges	**1**	**2**	**3**	AB
H4	Mulliken	−0.093	−0.095	−0.088	−0.077
	NBO	−0.063	−0.065	−0.059	−0.054
H5	Mulliken	−0.116	−0.122	−0.088	−0.077
	NBO	−0.076	−0.077	−0.059	−0.054
H6	Mulliken	−0.115	−0.091	−0.105	−0.077
	NBO	−0.075	−0.061	−0.078	−0.054
(H4 + H5 + H6)/3	Mulliken	−0.108	−0.103	−0.094	−0.077
	NBO	−0.071	−0.068	−0.065	−0.054

(H4 + H5 + H6/3, δ = −0.108) was found to be 40% more negatively charged (Table 2). Likewise, the T3EGDE and DEGDE additives increased the B–H charge by 34% and 22%, respectively. The enhanced hydricity of AB in the presence of the added promoters is also pronounced in NBO population analyses. The average charge ((H4 + H5 + H6)/3, δ = −0.071) of the hydridic B–H bonds in **1** is calculated to be 31% more negative than that of AB (δ = −0.054). Other polyetheral promoters produced more negatively charged B–H bonds than those of pristine AB (Table 2). These results strongly suggest that the charge transfer from oxygen atoms of a polyetheral promoter to AB through hydrogen bonding interactions induces the partial activation of B–H bonds. Note that in both analyses, the calculated B–H charges of **1–3** increased as the number of oxygen atoms increased (**1** > **2** > **3**).

An important question is then: how does the enhanced hydricity of **1** (or other AB–promoter adducts) *via* hydrogen bonding interaction promote the rate of AB dehydrogenation? The formation of DADB ($[H_3NBH_2NH_3]^+[BH_4]^-$) has previously been proposed to be an initial, key process for enhancing AB dehydrogenation.[12,41–43,53,54] In the proposed mechanism of AB dehydrogenation, two AB molecules interacted with each other to generate DADB following the formation of the new phase AB.[55] More recently, the influence of ammonium functionality (NH_4^+) on the rate of AB dehydrogenation was demonstrated by the addition of NH_4Cl to AB, which increased the rate of H_2-release.[12] Moreover, the addition of trace amounts of DADB to pristine AB has been reported to reduce the induction period or onset temperature for H_2-release.[12] In addition, Sneddon and coworkers found that an ionic liquid, 1-butyl-3-methyl imidazolium chloride (bmimCl), significantly enhanced the rate of H_2-release from a mixture of AB and bmimCl (50 : 50, wt%).[34] The authors found that the ionic liquid facilitated the formation of DADB in the highly polar medium, which improved the rate of H_2-release from AB. In a similar but different way, the chemical promoters employed in this study partially activate B–H bonds of AB to render B–H bonds more hydridic than those of AB without promoters. The partially activated B–H bonds through hydrogen bonding interaction could then play a pivotal role in enhancing the formation of DADB by transferring one of the more negatively charged hydrides into the boron atom of a neighboring AB (*vide infra*), ultimately accelerating the rate and extent of H_2-release from the AB mixtures.

Dixon and coworkers[39] computationally followed possible pathways for the formation of DADB from 2AB in the gas phase,

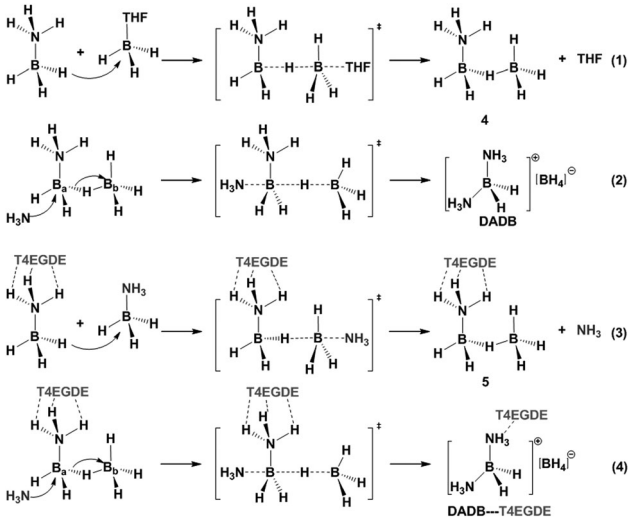

Fig. 8 A proposed mechanism involving interaction between AB and T4EGDE, leading to DADB.

which involved an initial hydride transfer reaction with the successive attack of ammonia. More recently, Shore and coworkers[56] proposed a mechanism for the formation of DADB involving an ammonia diborane ($NH_3BH_2(\mu\text{-}H)BH_3$) intermediate (**4**), based on ^{11}B NMR spectroscopy and DFT methods. The initial process for the formation of DADB was again proposed to be a hydride transfer reaction (eqn (1), Fig. 8). The formed $NH_3BH_2(\mu\text{-}H)BH_3$ species then reacted with NH_3 to give DADB (eqn (2), Fig. 8).[56] Likewise, an AB–promoter adduct can undergo a similar hydride transfer reaction to generate DADB (eqn (3) and (4), Fig. 8). In particular, the increased hydricity of the B–H bonds at **1** with hydrogen bonding interactions may lower the activation barrier for the hydride transfer reaction (eqn (3)). This hypothesis may also be supported by a recent report[57] for metal-free hydrogen transfers; Manners and coworkers demonstrated that an amine borane, $Me_2NH–BH_3$ delivered hydrogen atoms into $iPr_2N{=}BH_2$ to produce cyclodiborazane $[Me_2N–BH_2]_2$ and $iPr_2NH–BH_3$. Kinetic studies along with DFT methods revealed that this hydrogen transfer process involved a concerted but asynchronous hydrogen transfer with the B-to-B hydride transfer being advanced.[57] Molecular orbital analyses further indicated that the highest occupied molecular orbitals (HOMOs) of **1** exhibited strong contributions from σ bonding orbitals of the hydridic B–H bonds (Fig. S6†). The enhanced initial rates of the H_2-release from AB with the added promoter could thus result mainly from the interactions between AB and a promoter.

To gain an insight into the influence of AB–promoter interactions on the formation of DADB, we followed plausible pathways for the formation of DADB with and without T4EGDE in the gas phase. The located transition state geometries with and without the T4EGDE promoter clearly show the hydride transfer processes from H–BH_2 of AB into the boron atom of adjacent AB (Fig. 9). The calculated energy for the **TS1** without a promoter was calculated to be 14.4 kcal mol^{-1} higher than that of AB + AB (Fig. 9, upper line) and this **TS1** energy is slightly higher than that (12.4 kcal mol^{-1})[38] calculated by a high-level

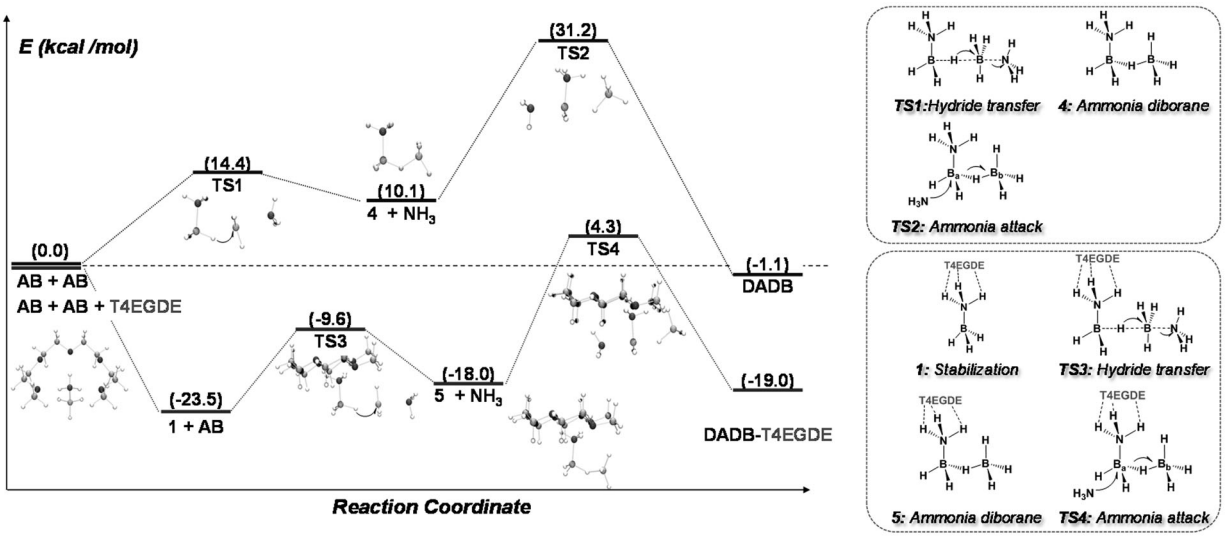

Fig. 9 Optimized intermediates and transition states for the formation of DADB in the presence of: (upper line) no promoter and (lower line) T4EGDE. Relative energies (parentheses) are in kcal mol^{-1}.

CCSD(T) calculation. In contrast, the reaction with 2AB and T4EGDE in the gas phase may initially give AB and AB·T4EGDE (**1**) species, followed by transferring one of the B–H hydrides into the neighboring AB. The corresponding **TS3** energy with T4EGDE was calculated to be 9.6 kcal mol^{-1} lower than that of AB + AB + T4EGDE (Fig. 9, lower line). The next process involves the nucleophilic attack of ammonia at one of the boron atoms (B_a) to produce DADB (eqn (2) and (4), Fig. 8). Note that two AB molecules would be formed upon incorporation of the ammonia molecule into B_b. The transition state (**TS2**) for this process without the promoter was calculated to be 31.2 kcal mol^{-1} higher than AB + AB (eqn (2)), close to that (32.1 kcal mol^{-1})[56] computed based on a high-level MP2 theory, whereas the computed energy for the corresponding transition state (**TS4**) with the T4EGDE promoter is 4.3 kcal mol^{-1} higher than that of AB + AB + T4EGDE (eqn (4)). These intermediates and transition states could further be stabilized by intermolecular dihydrogen bonding interactions with neighboring AB molecules.[56] This result strongly supports the hypothesis that the added promoter helps accelerate the formation of DADB by hydrogen bonding interactions.

Since these results obtained by theoretical methods predict that the T4EGDE promoter can induce the formation of DADB from AB even at a low temperature, we further examined the stability of the mixture of AB with T4EGDE (AB : T4EGDE = 4.0 : 0.23, molar ratio) at a low temperature of 50 °C using *in situ* solid state ^{11}B MAS-NMR spectroscopy. As depicted in Fig. 10a, no changes were observed upon heating the pristine AB solids at 50 °C for 180 min. In contrast, the new phase AB (δ = −23 ppm)[55] was readily formed from the mixture of AB and T4EGDE, leading to the formation of DADB after 50 min at 50 °C (Fig. 10b). In a separate experiment, a AB–T4EGDE mixture (AB : T4EGDE = 4.0 : 2.0, mmol) was stored at room temperature under a N_2 atmosphere and the sample was then characterized by the ^{11}B NMR spectroscopy after 11 days. The NMR studies revealed that the DADB species was formed even at room temperature after 11 days along with the production of H_2 (Fig. S7†), whereas the pristine AB solids were found to be much more stable at room temperature.

The previously proposed mechanism[12,42,43,53,54] involving the reactive DADB intermediate for the thermally-induced dehydrogenation of AB can thus be extended with the polyetheral promoters (Fig. 11). The hydrogen bonding interactions can induce more negatively charged B–H bonds of AB·T4EGDE (**1**) with stabilization, which then promote the formation of the reactive intermediate, DADB, to ultimately facilitate the release of the first equivalent of H_2 during AB dehydrogenation. This mechanistic pathway can also explain the observed inhibitory effect on AB dehydrogenation upon utilization of an excess amount of the T4EGDE promoter (Fig. 4). Statistically, most of the N–H bonds of AB would interact with oxygen atoms in the presence of excess additives. The resulting low concentration of free N–H bonds at AB would suppress the intermolecular dehydrogenation where free N–H and B–H bonds are needed.

Conclusions

Thermolytic dehydrogenation of AB is known to release hydrogen *via* a number of different pathways depending on promoters or catalysts used.[58] In this study, mixtures of AB and a polyetheral promoter with the weight ratio of 71 : 29 were initially utilized to produce hydrogen for practical fuel cell applications, and the H_2-release properties from the AB–promoter mixtures with different mole ratios were further examined. The polyetheral additives proved to be reasonably decent promoters for AB dehydrogenation. In particular, a small quantity of T4EGDE was found to enhance the extent and rate of H_2-release from AB at 85 °C *via* the formation of DADB assisted by the AB–promoter interactions, as supported by DFT methods and *in situ* solid state ^{11}B MAS-NMR spectroscopy. Compared to those suggested by

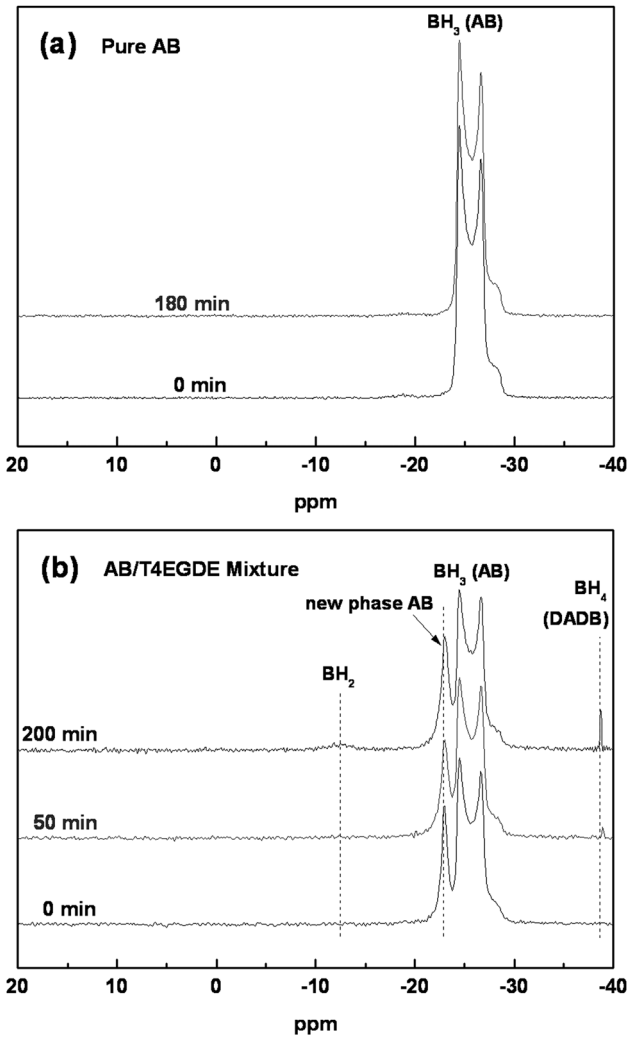

Fig. 10 *In situ* solid state $^{11}B\{^1H\}$ MAS-NMR spectra with time: (a) Pristine AB and (b) a mixture of AB and T4EGDE (AB : T4EGDE = 4.0 : 0.23, molar ratio). Samples were constantly heated at 50 °C.

previous studies,[12–34] this system has the unique feature of partially activating B–H bonds with nonmetal promoters; *i.e.*, the hydrogen bonding interactions likely play a pivotal role in facilitating the formation of DADB, thus enhancing the liberation of the first equivalent of H_2 from AB. Although a mechanism for the release of the second equivalent of H_2 from AB is still ambiguous, to the best of our knowledge, our study offers an extended understanding for the facilitated H_2-release from AB in the presence of polyetheral promoters. The metal-free H_2-release from AB with polyethers presented herein provides useful insights to develop efficient hydrogen storage systems for a number of long-term fuel cell applications.

Experimental

Materials

Polyetheral promoters including ethylene glycol dimethyl ether (EGDE), diethylene glycol dimethyl ether (DEGDE), triethylene glycol dimethyl ether (T3EGDE), and tetraethylene glycol dimethyl ether (T4EGDE) were purchased from Sigma Aldrich and used as-received. The structures of these promoters are depicted in Chart 1. Ammonia borane (AB, Aviabor, 98%) was ground into fine powder using a commercial grinder. Unless otherwise noted, all chemicals were stored and handled under an inert atmosphere of nitrogen.

Dehydrogenation of AB with added polyetheral promoters

In a typical experiment, AB was mixed with polyetheral promoters (EGDE, DEGDE, T3EGDE, or T4EGDE) at room temperature. Dehydrogenation reactions of the mixtures of AB and a promoter were conducted in modified glasswares (40 mL) with two necks. The reactor was purged with N_2 for 30 min before AB dehydrogenation reactions. The reactor was then immersed in a silicon oil bath preheated to a desired temperature (*e.g.*, 85 °C) upon vigorous stirring with a stirring rate of 300 rpm. The produced gases were

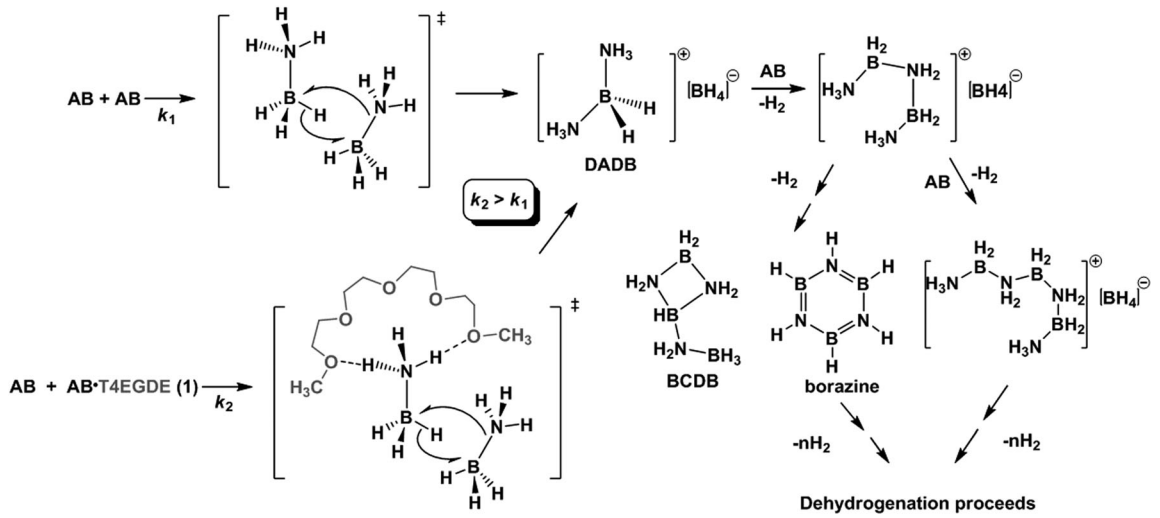

Fig. 11 A plausible pathway for the H_2-release from AB with T4EGDE, extended from the previously proposed mechanism[12,42,43,53,54] involving the reactive DADB intermediate.

initially delivered into a purification system filled with H_2O and T4EGDE traps maintained at 0 °C to remove gaseous byproducts except hydrogen, and the purified H_2 gas was then supplied to a gas burette system (Fig. S8†) for real-time measurements of H_2-release rates. For the *in situ* FT-IR experiments, the H_2O and T4EGDE traps were not used in order to detect gaseous byproducts. To examine the effect of a trace quantity of H_2O on AB dehydrogenation, 5 mg of H_2O was intentionally added into AB (0.12 g), followed by thermolysis at 85 °C with the H_2-measurements described above in a separate experiment, indicating that the dehydrogenation rate of the mixture was nearly identical with that of the pristine AB solid (Fig. S9†). Detailed experimental conditions about the weight and molar ratios between AB and a promoter for Fig. 1 and 4 are summarized in Tables S1 and S2, respectively, in the ESI.†

Physical measurements

The qualitative analyses of the gaseous byproducts were performed *in situ* during AB dehydrogenation at a constant temperature of 85 °C or increased temperatures of 85–105 °C using a FT-IR spectrometer (Nicolet iS10, Thermo Scientific) equipped with a MCT detector and a customized gas cell as well as using a FT-IR spectrometer (Infinity Gold, Mattson) equipped with a DTGS detector and a customized gas cell. Spectral data were collected using a scan rate of 16 scans min^{-1} with a resolution of 4 cm^{-1}. The evolution of the FT-IR spectra was recorded with a time interval of 10 min.

Waste-fuels (residues) in the reactor were extracted by dissolving in T4EGDE (0.5 g), followed by analysis using the ^{11}B NMR spectrometer (600 MHz FT-NMR, Varian). All ^{11}B NMR chemical shifts were referenced to BF_3OEt_2 (δ = 0.00 ppm). The solid state MAS-NMR measurements were performed *in situ* using a Bruker Avance 500 MHz spectrometer with a wide bore 11.7 T magnet and equipped with a boron-free Bruker 4 mm WVT (wide variable temperature) MAS probe. The resonance frequencies were 500.2 MHz and 160.2 MHz for proton (^1H) and boron (^{11}B) nuclei, respectively. The samples were packed into a 4 mm ZrO_2 rotor (Bruker) in an argon atmosphere glove box and sealed with a tight fitting Vespel Drive Cap (Bruker). Dry nitrogen gas was used for sample spinning in order to minimize oxidation from moisture or air contact. Sample heating was performed by running the bearing air through a heating coil, which was controlled by a Bruker BVTB 3500 temperature-controller unit. All ^{11}B NMR chemical shifts obtained by the solid state MAS NMR experiments were referenced to BF_3OEt_2 (δ = 0.00 ppm) externally. All proton decoupled, Bloch decay $^{11}B\{^1H\}$ spectra were recorded using a 0.5 s/12 pulse, with 80 kHz decoupling power, and a 10 s pulse delay under 8 kHz of sample spinning.

Computational methods

Density functional theory (DFT) and second order Møller–Plesset perturbation theory (MP2) calculations were performed using the Gaussian 09 program package[59] at Korea Institute of Science and Technology Information (KISTI). All ground-state and transition-state geometries were fully optimized at the B3LYP/6-31+G(d,p) level without any symmetry constraints. Harmonic vibrational frequency analyses were computed using the optimized geometries at the same level of theory to characterize the nature of stationary points. True stationary points on the potential energy surface had no imaginary frequency while true transition states possessed only one imaginary frequency. The identified normal mode possessing the imaginary vibrational frequency proposed the formation of the desired reactant and product (eqn (1)–(4); Fig. 9). Natural bond orbital (NBO) analyses were used to evaluate the atomic charge of the optimized geometries at the B3LYP/6-31+G(d,p) level. Since the B3LYP functional commonly underestimates the hydrogen bonding strength compared to the MP2 method,[60–62] all ground-state and transition-state energies were computed on the DFT-optimized geometries in vacuum using MP2 theory in conjunction with the 6-31++G(d,p) basis set, based on a recent report[56] associated with the formation of DADB. The zero-point vibrational energies were computed at the B3LYP/6-31+G(d,p) level and then scaled.[63] All reported MP2 energies are electronic energies with scaled zero-point energy corrections. The MP2 energies of the relevant intermediates and transition states for the formation of DADB are given in Fig. 9 and Table S4.†

Acknowledgements

This research was supported by Korea Institute of Energy Technology Evaluation and Planning (KETEP) of the Ministry of Knowledge Economy (MEST) (the New Renewable Energy Program, No. 20113030040020). Part of this research was also supported by the National Research Foundation of Korea Grant funded by the Korean Government (MSIP) (2013, University-Institute cooperation program). The NMR facility at Caltech was supported by the National Science Foundation (NSF) under Grant Number 9724240 and partially supported by the MRSEC Program of the NSF under Award Number DMR-520565. We are grateful to Professor Larry Sneddon and Dr Tom Autrey for their valuable comments.

Notes and references

1 Energy and Transportation: Challenges for the Chemical Sciences in the 21st Century, Organizing Committee for the Workshop on Energy and Transportation, The National Academies Press, Washington, D.C., 2003.
2 The Hydrogen Economy: Opportunities, Costs, Barriers and R&D Needs, Committee on Alternatives and Strategies for Future Hydrogen Production and Use, The National Academies Press, Washington, D.C., 2004.
3 B. C. H. Steele and A. Heinzel, *Nature*, 2001, **414**, 345.
4 DOE Targets for Onboard Hydrogen Storage Systems for Light-Duty Vehicles; http://www1.eere.energy.gov/hydrogenandfuelcells/storage/pdfs/targets_onboard_hydro_storage.pdf.
5 J. Yang, A. Sudik, C. Wolverton and D. Siegelwa, *Chem. Soc. Rev.*, 2010, **39**, 656.

6 S. Satyapal, J. Petrovicb, C. Read, G. Thomas and G. Ordaza, *Catal. Today*, 2007, **120**, 246.
7 Y. Kim, Y. Kim, S. Yeo, K. Kim, K. J.-E. Koh, J.-E. Seo, S. J. Shin, D.-K. Choi, C. W. Yoon and S. W. Nam, *J. Power Sources*, 2013, **229**, 170.
8 Y. Kim, C. W. Yoon, W.-S. Han, S. O. Kang and S. W. Nam, *Int. J. Hydrogen Energy*, 2012, **37**, 3319.
9 S. J. Kim, J. Lee, K. Y. Kong, C. R. Jung, I.-G. Min, S.-Y. Lee, H.-J. Kim, S. W. Nam and T.-H. Lim, *J. Power Sources*, 2007, **170**, 412.
10 A. D. Sutton, A. K. Burrell, D. A. Dixon, E. B. Garner, J. C. Gordon, T. Nakagawa, K. C. Ott, J. P. Robinson and M. Vasiliu, *Science*, 2011, **331**, 1426.
11 F. Mertens, G. Wolf and F. Baitalow, Ammonia borane and related compounds as hydrogen source materials, in *Handbook of Hydrogen Storage*, ed. M. Hirscher, Wiley-VCH Verlag GmbH & Co. KGaA, Weinheim, Copyright, 2010, ISBN: 978-3-527-32273-2.
12 D. J. Heldebrant, A. Karkamkar, N. J. Hess, N. J. Bowden, S. Rassat, F. Zheng, K. Rappe and T. Autrey, *Chem. Mater.*, 2008, **20**, 5332.
13 C. A. Jaska, K. Temple, K. Lough and I. Manners, *Chem. Commun.*, 2001, 962.
14 M. C. Denney, V. Pons, T. J. Hebden, D. M. Heinekey and I. Goldberg, *J. Am. Chem. Soc.*, 2006, **128**, 12048.
15 I. Göttker-Schnetmann, P. White and M. Brookhart, *J. Am. Chem. Soc.*, 2004, **126**, 1804.
16 K. W. Böddeker, S. G. Shore and R. K. Bunting, *J. Am. Chem. Soc.*, 1966, **88**, 4396.
17 T. J. Hebden, T. J. Denney, V. Pons, P. M. B. Piccoli, T. F. Koetzle, A. J. Schultz, W. Kaminsky, K. I. Goldberg and D. M. Heinekey, *J. Am. Chem. Soc.*, 2008, **130**, 10812.
18 A. Paul and C. B. Musgrave, *Angew. Chem., Int. Ed.*, 2007, **46**, 8153.
19 N. Blaquiere, S. Diallo-Garcia, S. I. Gorelsky, D. A. Black and K. Fagnou, *J. Am. Chem. Soc.*, 2008, **130**, 14034.
20 M. Käss, A. Friedrich, M. Drees and S. Schneider, *Angew. Chem., Int. Ed.*, 2009, **48**, 905.
21 T. Li, R. Churlaud, A. J. Lough, K. Abdur-Rashid and R. H. Morris, *Organometallics*, 2004, **23**, 6239.
22 S. E. Clapham, A. Hadzovic and R. H. Morris, *Coord. Chem. Rev.*, 2004, **248**, 2201.
23 K. Abdur-Rashid, S. E. Clapham, A. Hadzovic, J. N. Harvey, A. J. Lough and R. H. Morris, *J. Am. Chem. Soc.*, 2002, **124**, 15104.
24 R. J. Keaton, J. M. Blacquiere and R. T. Baker, *J. Am. Chem. Soc.*, 2007, **129**, 1844.
25 X. Yang and M. B. Hall, *J. Am. Chem. Soc.*, 2008, **130**, 1798.
26 M. B. Zimmerman, A. Paul, A. Zhang and C. B. Musgrave, *Angew. Chem., Int. Ed.*, 2009, **48**, 2201.
27 P. M. Zimmerman, A. Paul and C. B. Musgrave, *Inorg. Chem.*, 2009, **48**, 5418.
28 R. T. Baker, J. C. Gordon, C. W. Hamilton, N. J. Henson, P.-H. Lin, S. Maguire, S. Murugesu, B. L. Scott and N. C. Smythe, *J. Am. Chem. Soc.*, 2012, **134**, 5598.
29 A. Gutowska, L. Li, L. Shin, C. M. Wang, X. S. Li, J. C. Linehan, J. C. Smith, B. D. Kay, B. Schmid, W. Shaw, M. Gutowski and T. Autrey, *Angew. Chem., Int. Ed.*, 2005, **44**, 3578.
30 D. Neiner, A. Karkamkar, J. C. Linehan, B. Arey, T. Autrey and S. M. Kauzlarich, *J. Phys. Chem. C*, 2009, **113**, 1098.
31 D. Neiner, D. Luedtke, A. Karkamkar, W. Shaw, J. Wang, N. D. Browning, T. Autrey and S. M. Kauzlarich, *J. Phys. Chem. C*, 2010, **114**(32), 13935.
32 D. W. Himmelberger, C. W. Yoon, C. W. Bluhm, P. J. Carroll and L. G. Sneddon, *J. Am. Chem. Soc.*, 2009, **131**, 14101.
33 W. C. Ewing, A. Marchione, D. W. Himmelberger, P. J. Carroll and L. G. Sneddon, *J. Am. Chem. Soc.*, 2011, **133**, 17093.
34 D. W. Himmelberger, L. R. Alden, M. E. Bluhm and L. G. Sneddon, *Inorg. Chem.*, 2009, **48**, 9883.
35 M. E. Bluhm, M. G. Bradley, R. Butterick III, U. Kusari and L. G. Sneddon, *J. Am. Chem. Soc.*, 2006, **128**, 7748.
36 H. J. Himmel and H. Schnöckel, *Chem.–Eur. J.*, 2002, **8**, 2397.
37 D. A. Dixon and M. Gutowski, *J. Phys. Chem. A*, 2005, **109**, 5129.
38 M. T. Nguyen, V. S. Nguyen, M. H. Matus, G. Gopakumar and D. A. Dixon, *J. Phys. Chem. A*, 2007, **111**, 679.
39 V. S. Nguyen, M. H. Matus, D. J. Grant, M. T. Nguyen and D. A. Dixon, *J. Phys. Chem. A*, 2007, **111**, 8844.
40 N. T. Stetson, Hydrogen Storage Overview; 2012. DOE Annual Merit Review and Peer Evaluation Meeting (May 15, 2012); http://www.hydrogen.energy.gov/pdfs/review12/st000_stetson_2012_o.pdf, p. 22.
41 W. J. Shaw, W. J. Linehan, N. K. Szymczak, D. J. Heldebrant, C. Yonker, D. M. Camaioni, R. T. Baker and R. T. Autrey, *Angew. Chem., Int. Ed.*, 2008, **120**, 7603.
42 A. C. Stowe, W. J. Shaw, J. C. Linehan, B. Schmid and T. Autrey, *Phys. Chem. Chem. Phys.*, 2007, **9**, 1831.
43 J. F. Kostka, R. Schellenberg, F. Baitalow, T. Smolinka and F. Mertens, *Eur. J. Inorg. Chem.*, 2012, 49.
44 C. W. Yoon, P. J. Carroll and L. G. Sneddon, *J. Am. Chem. Soc.*, 2009, **131**, 855.
45 V. Pons, R. T. Baker, N. K. Szymczak, D. J. Heldebrant, J. C. Linehan, M. H. Matus, D. J. Grant and D. A. Dixon, *Chem. Commun.*, 2008, 6597.
46 NIST Material Measurement Laboratory, ammonia gas phase infrared spectrum; http://webbook.nist.gov/cgi/cbook.cgi?ID=C7664417&Type=IR-SPEC&Index=1.
47 H_2 storage capacity was calculated by the following equation, H_2 storage capacity (wt%, material based) = (weight of H_2 produced)/weight of reactants (AB + promoter).
48 H. M. Colquhoun, G. Jones, J. M. Maud, J. M. Stoddart and D. J. Williams, *J. Chem. Soc., Dalton Trans.*, 1984, 63.
49 D. R. Alston, J. F. Stoddart, J. B. Wolstenholme, B. L. Allwood and D. J. Williams, *Tetrahedron*, 1985, **41**, 2923.
50 B. Zhong, L. Song, X. X. Huang, L. Xia and G. Wen, *Phys. Scr.*, 2012, **86**, 015606.
51 N. Vinh-Son, S. Swinnen, M. H. Matus, M. H. Nguyen and D. A. Dixon, *Phys. Chem. Chem. Phys.*, 2009, **11**, 6339.
52 H. Wu, W. Zhou and T. Yildirim, *J. Am. Chem. Soc.*, 2008, **130**, 14834.

53 Z. Fang, J. Luo, X. Kang, H. Xia, S. Wang, S. Wen, X. Zhou and P. Wang, *Phys. Chem. Chem. Phys.*, 2011, **13**, 7508.
54 T. Autrey, M. Bowden and A. Karkamkar, *Faraday Discuss.*, 2011, **151**, 157.
55 W. J. Shaw, M. Bowden, A. Karkamkar, C. J. Howard, D. J. Heldebrant, N. J. Hess, J. C. Linehan and T. Autrey, *Energy Environ. Sci.*, 2010, **3**, 796.
56 X. Chen, X. Bao, J.-C. Zhao and J.-C. Shore, *J. Am. Chem. Soc.*, 2011, **133**, 14172.
57 E. M. Leitao, N. E. Stubbs, A. P. M. Robertson, H. Helten, R. J. Cox, G. C. Lloyd-Jones and I. Manners, *J. Am. Chem. Soc.*, 2012, **134**, 16805.
58 A. Staubitz, A. P. M. Robertson and I. Manners, *Chem. Rev.*, 2010, **110**, 4079. References therein.
59 M. J. Frisch, G. W. Trucks, H. B. Schlegel, G. E. Scuseria, M. A. Robb, J. R. Cheeseman, G. Scalmani, V. Barone, B. Mennucci, G. A. Petersson, H. Nakatsuji, M. Caricato, X. Li, H. P. Hratchian, A. F. Izmaylov, J. Bloino, G. Zheng, J. L. Sonnenberg, M. Hada, M. Ehara, K. Toyota, R. Fukuda, J. Hasegawa, M. Ishida, T. Nakajima, Y. Honda, O. Kitao, H. Nakai, T. Vreven, J. A. Montgomery, Jr., J. E. Peralta, F. Ogliaro, M. Bearpark, J. J. Heyd, E. Brothers, K. N. Kudin, V. N. Staroverov, R. Kobayashi, J. Normand, K. Raghavachari, A. Rendell, J. C. Burant, S. S. Iyengar, J. Tomasi, M. Cossi, N. Rega, J. M. Millam, M. Klene, J. E. Knox, J. B. Cross, V. Bakken, C. Adamo, J. Jaramillo, R. Gomperts, R. E. Stratmann, O. Yazyev, A. J. Austin, R. Cammi, C. Pomelli, J. W. Ochterski, R. L. Martin, K. Morokuma, V. G. Zakrzewski, G. A. Voth, P. Salvador, J. J. Dannenberg, S. Dapprich, A. D. Daniels, Ö. Farkas, J. B. Foresman, J. V. Ortiz, J. Cioslowski and D. J. Fox, *Gaussian 09, Revision A.1*, Gaussian, Inc., Wallingford, CT, 2009.
60 K. Kim and K. D. Jordan, *J. Phys. Chem.*, 1994, **98**, 10089.
61 S. Tsuzuki and H. P. Lüthi, *J. Chem. Phys.*, 2001, **114**, 3949.
62 J. Ireta, J. Neugebauer and M. Scheffler, *J. Phys. Chem. A*, 2004, **108**, 5692.
63 J. P. Merrick, D. Moran and L. Radom, *J. Phys. Chem. A*, 2007, **111**, 11683.

